Lawrence Berkeley National Laboratory

Lawrence Berkeley National Laboratory

Title

On the Baryonic Density and Susceptibilities in a Holographic Model of QCD

Permalink

https://escholarship.org/uc/item/5tw6t50j

Author

Kim, Keun-young

Publication Date

2009-11-11

Peer reviewed

eScholarship.org Powered by the California Digital Library
University of California

arXiv:0906.2978v1 [hep-th] 16 Jun 2009

On the Baryonic Density and Susceptibilities in a Holographic Model of QCD

Keun-young Kim[a], Jinfeng Liao[b]

[a]*Department of Physics & Astronomy, SUNY Stony Brook, NY 11794, USA.*
[b]*Nuclear Science Division, Lawrence Berkeley National Laboratory, MS70R0319, 1 Cyclotron Road, Berkeley, CA 94720, USA.*

Abstract

In this paper, we calculate analytically the baryonic density and susceptibilities, which are sensitive probes to the fermionic degrees of freedom, in a holographic model of QCD both in its hot QGP phase and in its cold dense phase. Interesting patterns due to strong coupling dynamics will be shown and valuable lessons for QCD will be discussed.

Key words: Holographic QCD, AdS/CFT, Baryonic Susceptibilities

1. Introduction

Historically string theory was developed during the attempt to build dual models for the strong interaction describing various hadrons and their scattering amplitudes [1]. After the advent of Quantum Chromodynamics (QCD) as the fundamental gauge theory of strong interaction, string theory departed into a quite different route with many fascinating discoveries. More recently, a new twist has been added to the story between string theory and QCD: the AdS/CFT correspondence [2, 3, 4], or more generally the gauge/gravity duality, has provided a way to study the strong coupling dynamics of non-Abelian gauge theories (like QCD) via its string theory dual in the much more tractable supergravity regime. A lot of interesting results have been achieved along this direction with applications in various aspects, for reviews see e.g. [5, 6, 7, 8, 9, 10, 11, 12].

While a specific gravity dual for real QCD hasn't been found yet, many important insights into the nonperturbative aspects of QCD have been obtained via gauge/gravity duality. Let's just mention two remarkable examples of such kind. Study of the so-called quark-gluon plasma (QGP), the deconfined phase of QCD at temperature higher than the deconfinement transition $T > T_c \approx 196MeV$ and low baryonic density, has been very important but proved to be rather difficult. Two powerful tools for such study include the lattice QCD and the heavy ion collisions experiments (e.g. at RHIC facility): interestingly, the former approach found that the the QGP thermodynamics (e.g. the energy density) deviates from Stefan-Boltzmann limit constantly by about 20% in the range $1.5-4T_c$ [13], while the latter approach found that the QGP produced at RHIC (corresponding to $1-2T_c$) has an extremely small shear viscosity to entropy density ratio η/s of the order 0.1 [14]. Both discoveries challenged naive expectation of a weakly coupled QGP right above T_c and led to the paradigm shift to a strongly coupled QGP (sQGP) [14, 15, 16]. It turns out that both results can be much better understood in light of the strong coupling results from gauge/gravity duality: the thermodynamics of CFT plasma at infinitely strong coupling has been calculated via its dual black hole to be exactly $\frac{3}{4}$ of the Stefan-Boltzmann limit [17], while a large class of strong coupling gauge theories with gravity dual have been shown to have their $\frac{\eta}{s} = \frac{1}{4\pi} \approx 0.08$. These successes have inspired a flush of activity to extract useful information for QCD and QGP via gauge/gravity duality, see e.g. reviews in [10, 11, 15].

In this paper, we focus on the fermionic sector i.e. the degrees of freedom

carrying baryonic charges in QCD thermodynamics, and use the gauge/gravity duality to qualitatively obtain some of their nonperturbative features. There are very rich dynamics associated with the quarks in QCD, for example the spontaneous chiral symmetry breaking in QCD vacuum and its restoration at high temperature/density. There are also interesting phase structures in the low T and high baryonic density region of QCD phase diagram where the fermionic sector becomes dominant. Color superconductivity [19] was found to occur at very high density with the phase presumably a color-flavor-locking one [20]. At moderately high density there are interesting phenomena like e.g. the interplay between the color superconductivity and chiral restoration and the pairing with mismatched Fermi surfaces [21][22]. More recently based on wisdom from large N_c argument, it has been proposed that there could be a new phase in the cold dense region, named "quarkyonic" phase [23][24], which is confined and yet has thermodynamics scaling as N_c like a system made of quarks. There are also many recent results on the baryonic density and susceptibilities from lattice QCD which show nonperturbative patterns [26, 27, 28, 29, 30].

It is thus of great interest to study these aspects of QCD with the handy tool of gauge/gravity duality. To this end, we use the Sakai-Sugimoto(SS) model [31], which have reproduced (at lease qualitatively) an impressive number of QCD results, for example: the baryon property, form factor [32], and the nuclear force [33], etc. The SS model has been studied at finite temperature [34] and at finite baryon density in [35, 36, 37]. We will particularly calculate the baryonic density and susceptibilities, which are sensitive probes to the fermionic degrees of freedom, from the Sakai-Sugimoto model both in the hot QGP phase and in the cold dense phase with the motivation to understand their patterns under strong coupling and find valuable lessons for QCD.

The paper is organized as follows. We give in Section.II a brief review of baryonic density and susceptibilities in QCD and in Section.III a brief review of pertinent Sakai-Sugimito results obtained before. The baryonic density and susceptibilities in Sakai-Sugimoto model will be analytically calculated for the hot QGP phase in Section.IV and for the cold dense phase in Section.V. Finally in Section.VI we summarize the results and discuss relevant lessons for QCD.

2. Brief Review of Baryonic Density and Susceptibilities in QCD

2.1. Definition and Examples

We start with a Taylor expansion of pressure $P(T,\mu)$ with respect to chemical potential μ (with the convention that quark carries unit baryonic charge) at fixed T:

$$P(T,\mu) = T^4 \sum_{n=0}^{\infty} \frac{d_n(T)}{n!} \left(\frac{\mu}{T}\right)^n \tag{1}$$

with the (dimensionless) baryonic susceptibilities $d_n(T)$ defined as

$$d_n(T) \equiv \frac{\partial^n (P/T^4)}{\partial(\mu/T)^n}\Big|_{\mu=0} \tag{2}$$

Note for the above d_n the odd-n ones vanish by symmetry. Furthermore we see all non-zero d_n except $n = 0$ represent certain contribution from the baryonic degrees of freedom, and importantly all non-baryonic degrees of freedom (e.g. the gluonic sector in QCD) do *not* directly contribute to them. So these derivatives probe the properties of the effective fermions in the system directly and sensitively. This can be seen also from the e.g. the baryonic density as given by

$$n_B(T,\mu) = T^3 \frac{\partial(P/T^4)}{\partial(\mu/T)} = T^3 \sum_{n=2}^{\infty} \frac{d_n(T)}{(n-1)!} \left(\frac{\mu}{T}\right)^{n-1} \tag{3}$$

To give an idea and to provide a benchmark of the baryonic density and susceptibilities, we explicitly evaluate these for a free gas of particles with mass M and baryonic charge B. The density is given by

$$n_B^{free}(T,\mu) = BN_i \frac{T^3}{2\pi^2} \int_0^{\infty} dx \left\{ \frac{x^2}{e^{\sqrt{(\beta M)+x^2}-(\beta B\mu)}+1} - \frac{x^2}{e^{\sqrt{(\beta M)+x^2}+(\beta B\mu)}+1} \right\} \tag{4}$$

with $\beta = 1/T$ and N_i denoting the number of internal degrees of freedom (e.g. color,flavor,spin, etc). The susceptibilities d_n can be obtained by subsequent differentiation with respect to μ. We are particularly interested in two limiting cases: the non-relativistic(NR) limit with $\beta M \to \infty$ and the ultra-relativistic(UR) limit with $\beta M \to 0$. In these limits we can obtain

concrete results below.

(i) NR limit: the baryonic density and susceptibilities in this limit are:

$$n_B^{free}\Big|_{NR} = BN_i \left(\frac{MT}{2\pi}\right)^{\frac{3}{2}} e^{-\frac{M}{T}} \left[e^{\frac{B\mu}{T}} - e^{-\frac{B\mu}{T}}\right] \tag{5}$$

$$d_n^{free}\Big|_{NR} = N_i \left(\frac{M}{2\pi T}\right)^{\frac{3}{2}} e^{-\frac{M}{T}} \times 2B^n \equiv \mathcal{F}\left[\frac{M}{T}\right] B^n \tag{6}$$

We observe two important points at this limit: (**a**) all susceptibilities d_n are *positive* and have the *same dependence on* T up to a constant coefficient ; (**b**) the ratio between successive susceptibilities is directly related to the baryonic charge carried by the degree of freedom, i.e. $d_{n+2}/d_n = B^2$, independent of M, T and n; (**c**) for multi-component non-interacting gas of species M_i, B_i, all d_n are simply a sum over species with the same formulae above and they remain all *positive*, but one then expect the ratios $d_{n+2}/d_n =< B_i^2 >$ to be an abundance-averaged baryonic charge which now depends on B_i and M_i, T, n as well.

(ii) UR limit: the baryonic density and susceptibilities in this limit are:

$$n_B^{free}\Big|_{UR} = N_i \frac{T^3}{6\pi^2}\left[B^4\left(\frac{\mu}{T}\right)^3 + \pi^2 B^2\left(\frac{\mu}{T}\right)\right] \tag{7}$$

$$d_2^{free}\Big|_{UR} = N_i\frac{B^2}{6} \quad , \quad d_4^{free}\Big|_{UR} = N_i\frac{B^4}{\pi^2} \quad , \quad d_{n>4}^{free}\Big|_{UR} = 0 \tag{8}$$

Again for multi-component non-interacting gas of species M_i, B_i, the d_n are simply a sum over species with the same formulae above. For such a Stefan-Boltzman gas of quarks (with $B_q = 1$ convention) with spin N_s, flavor N_f and color N_c, the susceptibilities per degrees of freedom (D.o.F) are simply $d_2^{SB}/(N_s N_f N_c) = \frac{1}{6}$, $d_4^{SB}/(N_s N_f N_c) = \frac{1}{\pi^2}$ with all higher ones vanishing.

In both limits of the free gas example above, we find all non-vanishing susceptibilities to be positive and proportional to B^n which implies the contribution of fermions with large B becomes larger and larger with increasing order n.

We end this part by emphasizing again that the density and susceptibilities are direct and sensitive probes to the fermions with baryonic charges in the system. In particular their deviation from the free patterns encodes important information about the dynamics and it is certainly of great interest to know the *behavior of baryonic density and susceptibilities under strong coupling*.

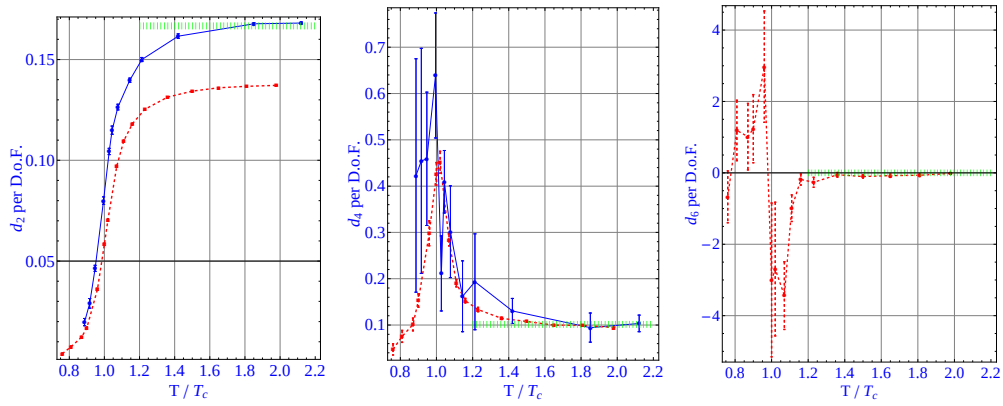

Figure 1: (from left to right) the susceptibilities d_2, d_4, and d_6 per D.o.F. calculated from lattice QCD. The dashed red lines in all panels are earlier 2-flavor results in [26] while the solid blue lines in d_2 and d_4 plots are recent 3-flavor results by the same group in [27]. The dotted green bands represent the Stefan-Boltzmann limit.

2.2. The Susceptibilities in Lattice QCD

While the susceptibilities contain very useful information about the fermionic degrees of fredom, it is generally hard to be calculated in a strongly coupled theory like QCD. Nevertheless such susceptibilities of QCD can be studied in its lattice formulation. In particular, calculating the d_n (defined at *zero* μ) offers an important method (via Taylor expansion) to explore the QCD phase diagram at finite density which was traditionally unaccessible for lattice QCD due to the well-known "sign problem". These susceptibilities are also directly related to baryonic charge fluctuations in the thermal QCD matter created in heavy ion collisions which can be experimentally measured [25]. The first lattice results for 2-flavor QCD [26] with a relatively large pion mass by Karsch et al from a few years ago showed highly nontrivial patterns near T_c, with strong deviation from the free case in the region $T \sim 1 - 2T_c$. More recent 3-flavor results with a more realistic pion mass by the same group [27] still preserved the nontrivial patterns close to T_c though with deviation from the free case limited to be below $\sim 1.4Tc$. See also other lattice works in e.g. [28][29][30] which all show similar behavior of the susceptibilities.

We now make a detailed discussion on these lattice results. Let's start with the $T < T_c$ part, i.e. the confined hadronic phase: in this phase we actually see from Fig.1 the same signs and similar T-dependence of $d_{2,4,6}$ (including exponential-like growth close to T_c) hinting at the NR limit of a free gas as in Eq.(6). And indeed a simple hadronic resonance gas model in-

cluding various baryons from the Particle Data Book can nicely fit the lattice data for $T < T_c$, see e.g. Fig.1 in [38]. In contrast, the data for $T > T_c$ do *not* resemble any free gas (NR or UR) model at all. A few nontrivial features are readily visible from Fig.1, especially for $1 - 1.4T_c$: *$d_{2,4,6}$ have rather distinctive patterns, with d_2 positive and mildly growing, d_4 positive and rapidly dropping, while d_6 negative and dropping even more abruptly.* The susceptibilities results clearly disfavor any weakly interacting quasiparticle models for the deconfined quark-gluon plasma (QGP) phase right above T_c, instead they indicate non-perturbative effect from strong coupling. This observation turns out to be consistent with the conclusion from other independent approaches that the QGP in the same $1-2T_c$-region is rather strongly coupled, now called sQGP. In particular the experimental study of the QGP phase by heavy ion collisions at RHIC suggests that it behaves as a very good liquid [14, 15, 16, 10]. Lattice works on e.g. thermodynamics [39] and transport properties [40], heavy quark potentials [41] and charmonium above T_c [42] also point to a similar conclusion. A microscopic explanation of such strong coupling results may rely on understanding of the specific mechanism of how the confinement occurs toward T_c from above: it has been suggested under the generic spirit of electric-magnetic duality that the QCD plasma close to T_c is actually a *magnetic* one, made of light and abundant monopoles which become Bose-condensed at T_c and enforce confinement [43, 44, 45, 46].

Returning to the non-trivial susceptibilities in $1-1.4T_c$, a theoretical understanding is still lacking. One particular suggestion involves possible bound states of quarks and gluons even in the plasma phase due to the presence of still strong coupling in $1 - 2T_c$ [47, 48, 49], including both conventional colorless states (remnants of mesons and baryons) and colored states like diquarks, q-g states and even polymer-like chains. Those bound states carrying baryonic charges can contribute substantially to the susceptibilities, as first pointed out by Liao and Shuryak in [38], and especially become more and more important in higher orders. To see this, one just notes that diquarks have baryonic charge $B = 2$ and baryons $B = 3$, and that the susceptibilities go like $d_n \sim B^n$ as evident from Eq.(6,8): this means even the density of the bound states may be small compared to quarks but they still can dominate e.g. d_4, d_6 and even higher order ones. It was shown in [38] that the bound states contribution, mainly from baryons, could be dominant for the peak and wiggle structures seen in the lattice data. This was confirmed by an even better agreement with data in later studies using the so-called PNJL model [50] in which due to Polyakov line suppression of colored states below

and around T_c, precisely the 3-quark colorless combinations (e.g. baryons) dominate the nontrivial susceptibilities around T_c. Despite these progresses, it is still unclear *how the strong coupling dynamics affects the susceptibilities from individual quarks* — this is what we attempt to address in the present paper.

To conclude this Section, we have seen that the baryonic density and susceptibilities are sensitive probes to the degrees of freedom carrying baryonic charges, and can exhibit rather nontrivial structures in strong coupling regime as shown by lattice QCD data. It is natural, then, to study these properties for strongly coupled gauge theories in general and for useful models of QCD in particular. To this end, the Sakai-Sugimoto model [31] is a good choice: as a holographic model of QCD, it is calculable in strong coupling regime by virtue of the gauge/string duality and has been shown to have many realistic features of QCD. In the rest of the paper, we will calculate the baryonic density and susceptibilities in the Sakai-Sugimoto model and discuss the lessons for QCD.

3. Brief Review of Sakai-Sugimoto Model with Chemical Potential

In this section we summarize the Sakai-Sugimoto (SS) model for notation and completeness. For a thorough presentation we refer [31] for zero temperature and [34] for finite temperature.

The SS model, in brief, is defined by the dynamics of N_f D8-$\overline{\text{D8}}$ branes in the background field (the metric, the dilaton, and the Ramond-Ramond field) generated by N_c D4-branes. In order not to disturb the background we require $N_f \ll N_c$, which is called the "probe" limit and corresponds to the quenched approximation. The low energy dynamics of D8-$\overline{\text{D8}}$ branes are governed by the Dirac-Born-Infeld (DBI) action and the Chern-Simons (CS) action:

$$S_{\rm DBI} = -T_8 \int d^9x \; e^{-\phi} \; \mathrm{tr} \sqrt{-\det(g_{MN} + 2\pi\alpha' F_{MN})} \; , \tag{9}$$

$$S_{\rm CS} = \frac{1}{48\pi^3} \int C_3 \mathrm{tr}\, F^3 \; , \tag{10}$$

where ϕ and C_3 are the dilaton and the Ramond-Ramond field. The metric generated by D4 brane is encoded in the induced metric g_{MN} on the D8-$\overline{\text{D8}}$ branes. $F_{MN} = \partial_M A_N - \partial_N A_M - i\,[A_M, A_N]$ $(M, N = 0, 1, \cdots, 8)$ are the

field strength tensor of the $U(N_f)$ gauge fields on the D8-branes. Note the tr is taken over the N_f-dimensional flavor space. $T_8 = \frac{1}{(2\pi)^8 l_s^9}$ is the tension of the D8-brane. In the following subsections we will specify the ingredient fields of the DBI and CS action: the induced metric, dilaton, RR field, and the gauge field.

3.1. Ingredient fields

The induced metric on the D8 branes from the D4 branes background metric can be written as [31, 34]

$$ds^2_{\rm D8} = g_{00}(dX_0^E)^2 + g_{xx}(d\vec{X})^2 + g_{UU}dU^2 + g_{SS}d\Omega_4^2 \ , \tag{11}$$

where[1]

$$g_{00} = \alpha\left(\frac{U}{R}\right)^{3/2},\ g_{xx} = \left(\frac{U}{R}\right)^{3/2},\ g_{UU} = \left(\frac{R}{U}\right)^{3/2}\gamma,\ g_{SS} = \left(\frac{R}{U}\right)^{3/2}U^2$$

$$\alpha \ \to \ 1 \ , \qquad \gamma \ \to \ \frac{1}{f(U)} + \left(\frac{\partial X_4}{\partial U}\right)^2\left(\frac{U}{R}\right)^3 f(U) \ , \quad \text{(Confined phase)}$$

$$\alpha \to f(U) \ , \quad \gamma \to \frac{1}{f(U)} + \left(\frac{\partial X_4}{\partial U}\right)^2\left(\frac{U}{R}\right)^3 \ . \qquad \text{(Deconfined phase)}$$

The embedding information is encoded only in γ and thereby g_{UU}. For definition of the warping factor $f(U)$ in both confined and deconfined phases, see the appendix.

The dilaton and RR field are given as

$$e^{\phi} = g_s\left(\frac{U}{R}\right)^{3/4} \ , \quad F_4 \equiv dC_3 = \frac{2\pi N_c}{\Omega_4}\epsilon_4 \ , \tag{12}$$

where g_S is the string coupling constant, $\Omega_4 = 8\pi^2/3$ is the volume of the unit S^4 and ϵ_4 is the corresponding volume form.

For the gauge field we only consider the time component of the $U(1)$ part of the $U(N_f)$ gauge field, which is normalized as

$$\frac{1}{\sqrt{2N_f}}\hat{A}_0(U) \ , \tag{13}$$

[1] In the appendix, the background metric and coordinate notation convention are shown.

where we also assumed the $\hat{A}_0$ is only a function of U. This choice of the *bulk* gauge field is a standard holographic way to introduce the chemical potential in the *boundary* field theory. $\hat{A}_0(\infty)$ of the classical solution is identified with the chemical potential.

3.2. The DBI action

the DBI action (9) reads

$$S_{\rm DBI} = N_s \cdot \Omega_4 \cdot T_8 \int dU e^{-\phi} g_{SS}^2 g_{xx}^{\frac{3}{2}} \sqrt{g_{00} g_{UU} - \left(2\pi\alpha' \hat{A}_0{}'\right)^2} \,, \tag{14}$$

where $N_s = 2$ and reflects the two contributions from D8 and $\overline{\rm D8}$ branes and Ω_4 results from the trivial angle integration of S^4. The symbol $'$ denotes the differentiation with respect to U. Note that $g_{00}g_{UU}$ is the only place where the confined and deconfined phases are distinguished.

In terms of the dimensionless variables defined as [36]

$$u = \frac{U}{R} \,, \quad x_4 = \frac{X_4}{R} \,, \quad \tau = \frac{X_0^E}{R} \,, \quad \hat{a} = \frac{2\pi\alpha' \hat{A}}{\sqrt{2N_f} R} \,, \tag{15}$$

the DBI action reads

$$S_{\rm DBI} = \mathcal{N} \int du u^4 \sqrt{f(u)(x_4'(u))^2 + \frac{1}{u^3}\left(\left\{ \begin{array}{c} \frac{1}{f(U)} \\ 1 \end{array} \right\} - (\hat{a}_0'(u))^2\right)} \quad \begin{array}{l} \text{confined} \\ \text{deconfined} \end{array} \,,$$

where

$$\mathcal{N} = \frac{N_s N_f T_8 R^5 \Omega_4 (\beta V_3)}{g_s} \,. \tag{16}$$

β is the inverse temperature, V_3 is the volume of $\vec{X}$ space.

For simplicity in this paper we only consider the antipodal configuration, in which the D8 branes and $\overline{\rm D8}$ branes are maximally separated at the boundary. This implies that, in the confined phase, the D8-$\overline{\rm D8}$ branes are connected at $U = U_{\rm KK}$, and, in the deconfined phase, D8 and $\overline{\rm D8}$ branes are parallel to each other extending to the black hole horizon. Since it also implies that x_4 is constant ($x_4' = 0$) the DBI action is reduced to

$$S_{\rm DBI} = \mathcal{N} \int du u^{\frac{5}{2}} \sqrt{\left\{ \begin{array}{c} \frac{1}{f(U)} \\ 1 \end{array} \right\} - (\hat{a}_0'(u))^2} \qquad \begin{array}{l} \text{confined} \\ \text{deconfined} \end{array} \,, \tag{17}$$

The antipodal configuration simplifies the problem since we only need to solve the one variable ($\hat{a}_0$) equation instead of the coupled equations of two variables ($\hat{a}_0$, x_4). It also simplifies the phase diagram of holographic QCD since there is no "cusp" configuration studied in [36]. Thus the deconfined phase at $T > T_c$ and any μ corresponds to the hot QGP phase, [2] and the confined phase at $T < T_c$ and sufficiently large $\mu > \mu_c$ corresponds to a cold dense phase made of baryonic matter while at small $\mu < \mu_c$ the phase is the trivial vacuum configuration with zero baryonic density. The onset chemical potential, μ_c, is defined in (26). The antipodal configuration will allow us to obtain analytic results for both the hot QGP phase and the cold dense phase, which shall remain qualitatively the same for large non-maximal separations of D8-$\overline{\text{D8}}$ branes.

3.3. Grand potential

The grand potential is identified with the on-shell DBI action. For convenience we will compute the rescaled grand potential defined as [3]

$$\Omega(t,\mu) = \frac{1}{\mathcal{N}} S_{\rm DBI}|_{\rm on-shell} \ , \tag{18}$$

where t is the dimensionless temparature and μ is the dimensionless chemical potential defined as

$$t = T \cdot R \ , \qquad \mu = \hat{a}_0(\infty) \ . \tag{19}$$

3.3.1. QGP phase

Let us first consider the deconfined phase,

$$S_{\rm DBI} = \mathcal{N} \int du u^{\frac{5}{2}} \sqrt{1 - (\hat{a}_0'(u))^2} \ . \tag{20}$$

Since $\hat{a}_0$ is a cyclic coordinate, its conjugate momentum is conserved, which is defined up to a normalization as

$$d \equiv -\frac{1}{\mathcal{N}} \frac{\delta S_{\rm DBI}}{\delta \hat{a}_0'(u)} = u^{\frac{5}{2}} \frac{\hat{a}_0'}{\sqrt{1 - (\hat{a}_0'(u))^2}} \ , \tag{21}$$

[2] In general there could also be other phases corresponding to connected configurations in deconfined phase as shown in [36].

[3] The grand potential in SS model has been computed in several papers [35, 36, 37] with various notational conventions. In this paper we follow the convention in [36].

and $\hat{a}_0$ is easily solved. Especially

$$\mu = a_0(\infty) = \int_{u_T}^{\infty} du \frac{d}{\sqrt{u^5 + d^2}} \ , \tag{22}$$

where $a(u_T) = 0$ for the regularity at the horizon. With this solution the grand potential reads

$$\Omega(t, \mu) = \int_{u_T}^{\infty} du \frac{u^5}{\sqrt{u^5 + d(\mu)^2}} \ , \tag{23}$$

where $d(\mu)$ is the function of μ via (22).

3.3.2. Cold dense phase

In the confined phase we can do the same analysis with

$$S_{\rm DBI} = \mathcal{N} \int du u^{\frac{5}{2}} \sqrt{f(u) - (\hat{a}_0'(u))^2} \ . \tag{24}$$

However in this case we need to consider the explicit source term. Contrary to the deconfined phase, D8 and $\overline{\rm D8}$ branes are connected at $u = u_{KK}$. For a nontrivial $\hat{a}_0$ there must be a singularity at $u = u_{KK}$ and to take this account we consider the D4 branes wrapping S^4 as the baryon source. The source of a uniform distribution of D4 branes ($\sim d$) can be explicitly introduced by the CS action. Referring to [36] for more detail, we simply quote the final result for the grand potential and chemical potential

$$\Omega(\mu) = \int_{u_{KK}}^{\infty} du \frac{1}{\sqrt{f(u)}} \frac{u^5}{\sqrt{u^5 + d(\mu)^2}} \ , \tag{25}$$

$$\mu = a_0(\infty) = \int_{u_{KK}}^{\infty} du \frac{1}{\sqrt{f(u)}} \frac{d}{\sqrt{u^5 + d^2}} + \mu_c \ . \tag{26}$$

where $\mu_c \equiv \frac{1}{3} u_{KK}$ is the onset chemical potential of the cold dense phase.

4. Baryonic Density and Susceptibilities in the QGP Phase

At $T > T_c$ the Saika-Sugimoto model has a deconfined, chirally symmetric QGP phase for any μ. We make use of the analytic results for QGP phase

to analyze its barynoic degrees of freedom. Using Eq.(23,22) and subtracting out the vacuum part in the grand potential, we explicitly write out the following equations as our starting point at given T, μ:

$$P_{QGP}\left[T, d(T,\mu)\right] = \left[\frac{2}{7}\Gamma_A d^{\frac{7}{5}} + \frac{2}{7}u_T(d^2+u_T^5)^{\frac{1}{2}} - \frac{2}{7}u_T d\ {}_2\mathbf{F}_1\left(\frac{1}{5},\frac{1}{2};\frac{6}{5};-\frac{u_T^5}{d^2}\right)\right] \tag{27}$$

$$\Gamma_A d^{\frac{2}{5}} - u_T\ {}_2\mathbf{F}_1\left(\frac{1}{5},\frac{1}{2};\frac{6}{5};-\frac{u_T^5}{d^2}\right) - \mu = 0\,, \quad \Gamma_A = \frac{\Gamma(\frac{3}{10})\Gamma(\frac{6}{5})}{\sqrt{\pi}} \tag{28}$$

In principle we need to solve $d(T,\mu)$ from the constraint and then obtain the full $P[T,\mu]$ to calculate density and susceptibilities. However, we can make use of the chain rule to do the calculation without solving the constraint. In other words, we (temporarily) consider μ as being determined by T, d:

$$\mu = \Gamma_A d^{\frac{2}{5}} - u_T\ {}_2\mathbf{F}_1\left(\frac{1}{5},\frac{1}{2};\frac{6}{5};-\frac{u_T^5}{d^2}\right) \tag{29}$$

And we first evaluate the derivatives over d:

$$\frac{\partial P}{\partial d} = \frac{2u_T}{3}\left(\frac{d^2}{u_T^5}\right)^{\frac{1}{2}}\ {}_2\mathbf{F}_1\left(\frac{3}{10},\frac{3}{2};\frac{13}{10};-\frac{d^2}{u_T^5}\right) \tag{30}$$

$$\frac{\partial \mu}{\partial d} = \frac{2u_T}{3d}\left(\frac{d^2}{u_T^5}\right)^{\frac{1}{2}}\ {}_2\mathbf{F}_1\left(\frac{3}{10},\frac{3}{2};\frac{13}{10};-\frac{d^2}{u_T^5}\right) \tag{31}$$

The density is then given by $n_B = \frac{\partial P/\partial d}{\partial \mu/\partial d} = d$, as it should. To determine its ultimate dependence on T, μ we will have to solve the constraint.

We now calculate the susceptibilities d_n as defined in Eq.(2). To do that we introduce $P_n(T,d) \equiv \frac{\partial P^n}{\partial \mu^n}$ with $d_n = t^{n-4}\cdot P_n(d\to 0)$ (noting that $d\to 0$ is equivalent to $\mu \to 0$). P_n can be evaluated order by order, using $P_{n+1} = \frac{\partial P_n/\partial d}{\partial \mu/\partial d}$. The final results to the order $n=10$ are given below:

$$\begin{aligned} d_{n=2,4,6,8,10} &= \chi_n\, u_T^{-n+7/2}\, t^{n-4} \qquad = \chi_n \left(\frac{4\pi}{3}\right)^{-2n+7} t^{-n+3} \\ \chi_2 = \frac{3}{2} \quad &, \quad \chi_4 = \frac{3^5}{2^3\cdot 13} \quad , \qquad \chi_6 = -\frac{3^8\cdot 5\cdot 31}{2^5\cdot 13^2\cdot 23} \quad , \\ \chi_8 = \frac{3^9\cdot 5^2\cdot 7\cdot 3011}{2^7\cdot 11\cdot 13^3\cdot 23} \quad &, \qquad \chi_{10} = -\frac{3^1 4\cdot 5^2\cdot 7\cdot 24546787}{2^9\cdot 11\cdot 13^4\cdot 23^2\cdot 43} \end{aligned} \tag{32}$$

These results show very distinctive patterns: (**a**) first of all we see simple power dependence on temperature but different orders depend on T very differently; (**b**) particularly, only d_2 has positive power of T-dependence, i.e. growing with T, while all higher order susceptibilities have negative power thus vanish in the $T \to \infty$ limit; (**c**) furthermore, we notice there is an alternating sign pattern for $n > 2$, i.e. $d_{4,8}$ are positive while $d_{6,10}$ are negative; (**d**) finally we notice the ratios between successive susceptibilities are $d_{n+2}/d_n \sim t^{-2}$. As is evident from the above results, even in the QGP phase with quarks as the basic baryonic charge carriers, the strong interaction modifies the behavior significantly, resulting in non-perturbative patterns of these susceptibilities.

At this point, it would be interesting to see the actual dependence of the susceptibilities on physical parameters by recovering all the dimensions (and neglected constants) of involved quantities, i.e. P, μ, T. This can be done via the following:

$$P \to P \times \left[\frac{N_s \cdot N_f \cdot N_c \cdot \lambda^3}{2^8 \cdot 3 \cdot \pi^5 \cdot M_{KK}^3 \cdot R^7}\right] \quad , \quad \mu \to \mu \times \left[\frac{\lambda}{4 \cdot \pi \cdot M_{KK} \cdot R^2}\right] \tag{33}$$

We also re-scale temperature by $t \equiv TR \to \frac{T}{T_c} \times [\frac{M_{KK} \cdot R}{2\pi}] \equiv \tilde{T} \times [\frac{M_{KK} \cdot R}{2\pi}]$. Eventually we arrive at the results below:

$$d_n = \xi_n \times N_s \times N_c \times N_f \times \left(\frac{1}{\lambda \tilde{T}}\right)^{n-3} \tag{34}$$

with $\xi_n = \chi_n \cdot 3^{2n-8}/(\pi \cdot 2^{n-3})$ (note the sign patterns of ξ_n follow from χ_n, i.e. $\xi_{2,4,8,\ldots} > 0$ while $\xi_{6,10,\ldots} < 0$). First of all we notice the degrees of freedom counting reflects quark-like dependence, as baryonic or any other non-single combinations of quarks would result in different dependence on both N_c *and* N_f. On the other hand we see nontrivial power dependence on the coupling: again $d_2 \sim \lambda \tilde{T}$ grows both with λ and $\tilde{T}$ but all higher susceptibilities will be *suppressed at very strong coupling*.

Finally let's discuss the asymptotic behavior of baryonic density at very large and very small density/chemical potential, i.e. $\mu \to \infty$ and $\mu \to 0$. In these limits we can solve the constraint equation to obtain the density.
(i) Dense Limit in QGP Phase: In the dense limit $\mu \to \infty$ and thus $d \to \infty$, we solve the constraint equation Eq.(28) to leading order and obtain the

pressure and baryonic density to be (after recovering physical dimensions):

$$\frac{P^{dense}}{T_c^4} \sim N_s \cdot N_f \cdot N_c \cdot \lambda^{-\frac{1}{2}} \left(\frac{\mu}{T_c}\right)^{\frac{7}{2}} \quad , \quad \frac{n_B^{dense}}{T_c^3} \sim \frac{7}{2} \cdot N_s \cdot N_f \cdot N_c \cdot \lambda^{-\frac{1}{2}} \left(\frac{\mu}{T_c}\right)^{\frac{5}{2}} \tag{35}$$

We can also calculate the energy per particle

$$\bar{E} \approx \frac{\mu n - P}{n} = \frac{5}{7}\,\mu = \frac{20}{21}\,\bar{E}_{S.B.} \tag{36}$$

with $E_{S.B.} = 3\mu/4$ representing the energy per particle for a free gas of massless fermions at zero temperature and finite μ. Amusingly, the strong coupling result misses the non-interacting limit by only $1/21 \sim 5\%$ despite the strong coupling dynamics.

(ii) Dilute Limit in QGP Phase: In the dilute limit $\mu \to 0$ and thus $d \to 0$, we note that $\left[{}_2\mathbf{F}_1\left(\frac{1}{5}, \frac{1}{2}; \frac{6}{5}; -\frac{u_T^5}{d^2}\right)\right]\Big|_{d\to 0} \to \Gamma_A \cdot \frac{d^{\frac{2}{5}}}{u_T} - \frac{2}{3}\frac{d}{u_T^{\frac{5}{2}}} + \hat{o}(d^2)$ and can then calculate the baryonic density to leading order

$$\frac{n_B^{dilute}}{T_c^3} \sim N_s N_f N_c \lambda \left(\frac{T}{T_c}\right)^3 \left(\frac{\mu}{T_c}\right) \tag{37}$$

This result has linear dependence on μ, in common with the leading order at small μ of free fermion gas at UR limit. The strong coupling density here however depends on coupling λ and also has T^3 dependence, differing from the free case which has no coupling and has T^2 dependence.

5. Baryonic Density and Susceptibilities in the Cold Dense Phase

We now turn to the cold dense phase at $T = 0$. To study this phase, we focus on the situation with maximal $D8$-$\bar{D}8$ separation which allows tractable analytic formulae and much simplifies the calculation. For non-maximal separation, the physics at $T = 0$ remains qualitatively the same while the calculation is much more involved.

We start with Eq.(25,26) and further rewrite the pressure and chemical potential as a function of d into the following forms by re-scaling the quantities with u_{KK}:

$$\tilde{P} = \frac{P}{(u_{KK})^{\frac{7}{2}}} = \int_1^\infty d\tilde{u} \frac{\tilde{u}^4}{\sqrt{\tilde{u}^3 - 1}} \left[\frac{1}{\sqrt{1 + \frac{\tilde{d}^2}{\tilde{u}^5}}} - 1\right] \tag{38}$$

$$\tilde{\mu} = \frac{\mu}{u_{KK}} = \tilde{\mu_c} + \int_1^\infty d\tilde{u} \frac{\tilde{u}^{\frac{3}{2}}}{\sqrt{\tilde{u}^3 - 1}} \sqrt{\frac{\tilde{d}^2}{\tilde{u}^5 + \tilde{d}^2}} \tag{39}$$

In the above $\tilde{d}^2 \equiv d^2/u_{KK}^5$ and $\tilde{\mu_c} = \mu_c/u_{KK} = 1/3$. Also note in the pressure we have subtracted out the vacuum part, e.g. the (-1) within the bracket. These can be easily solved numerically: for each given $\tilde{\mu}$ we can first solve $\tilde{d}$ from Eq.(39) and then obtain $\tilde{P}$ from Eq.(38), and the results are shown as solid blue lines in Fig.2.

A few comments are in order. First we notice that for $\tilde{\mu} < \tilde{\mu_c}$ there is no solution for $\tilde{d}$ as is evident from Eq.(39), so the solution is the trivial U-shape and the system is in vacuum phase without any dependence on $\tilde{\mu}$. When $\tilde{\mu} > \tilde{\mu_c}$ baryons start to emerge and a new phase with nonzero baryonic density takes over the vacuum one. Furthermore both the pressure and the baryonic density are continuous at $\tilde{\mu_c}$ transition while the first derivative of $\tilde{d}$ versus μ (i.e. the lowest susceptibility at $\tilde{\mu_c}$) is not, which implies a second order phase transition. In physical unit, one has $\mu_c = \frac{\lambda M_{KK}}{27\pi} = \frac{2}{27} \times \lambda \times T_c$: with $\lambda \sim 20 - 50$, the relation reasonably agrees with current rough estimate of μ_c/T_c in QCD.

We now make an expansion of the pressure and density in the cold dense phase close to $\tilde{\mu_c}$. This can be done by systematically analyze the expansion of $\tilde{d} \to 0$ order by order in the integrands of Eqs.(38,39). The result for the pressure is:

$$\begin{aligned} \tilde{P} \quad &= \sum_n c_{2n} \left(\tilde{\mu} - \tilde{\mu_c}\right)^{2n} \qquad (40) \\ c_2 \quad &= \frac{3}{2\pi}\,,\ c_4 = \frac{9\,\Gamma\left(\frac{13}{6}\right)}{\pi^{\frac{7}{2}}\,\Gamma\left(\frac{11}{3}\right)}\,,\ c_6 = \frac{243}{16\pi^6}\left[\frac{2\,\Gamma\left(\frac{13}{6}\right)^2}{\Gamma\left(\frac{8}{3}\right)^2} - \frac{\sqrt{\pi}\,\Gamma\left(\frac{23}{6}\right)}{\Gamma\left(\frac{13}{3}\right)}\right]\,,\ \ldots \end{aligned}$$

We skip to show the higher order coefficients whose expressions become really long. Here we give an idea of the numbers: $c_2 = 0.477465, c_4 = 0.0441772, c_6 = 0.001576, c_8 = -0.000365984, c_{10} = 0.0000107106$. These coefficients can be directly related to baryonic susceptibilities defined at $\tilde{\mu} = \tilde{\mu_c}$, i.e.:

$$D_{2n} \equiv \frac{\partial^{2n}(P/\mu_c^4)}{\partial(\mu/\mu_c)^{2n}}\Big|_{\mu=\mu_c} = \frac{\tilde{\mu_c}^{2n-4}}{u_{KK}^{\frac{1}{2}}} \frac{\partial^{2n}\tilde{P}}{\partial\tilde{\mu}^{2n}}\Big|_{\mu=\mu_c} = \frac{\tilde{\mu_c}^{2n-4}}{u_{KK}^{\frac{1}{2}}}\,(2n)!\,c_{2n} \tag{41}$$

In Fig.2(left) we compare the full numerical result (solid blue line) of the pressure with its Taylor series results truncated at the 1st(red), 2nd(green),

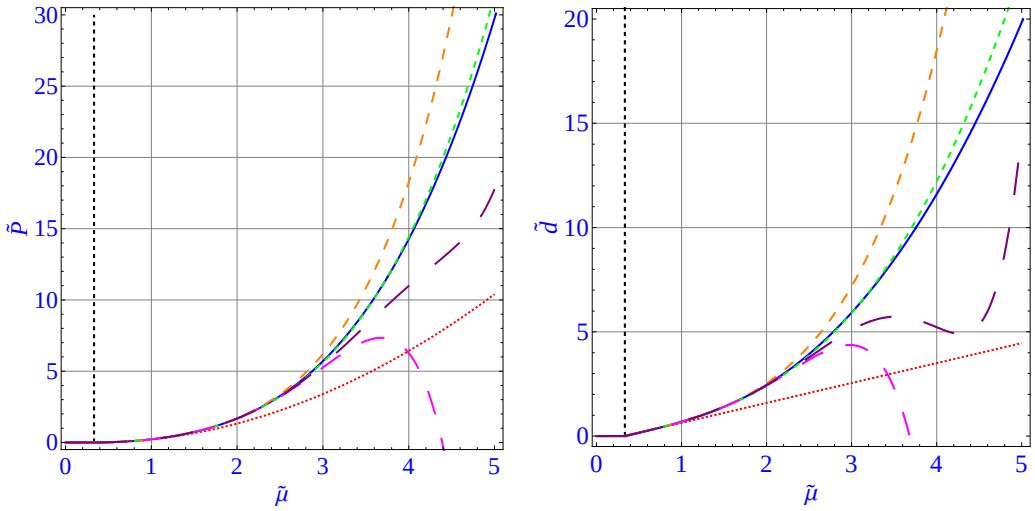

Figure 2: Comparison of the full numerical results(solid blue line) for the pressure(left) and density(right) with their respective Taylor series results(dashed lines with growing lengths) truncated at the 1st(red), 2nd(green), 3rd(orange), 4th(magenta), and 5th(purple) order. The vertical dashed black line indicates the position of the phase transition.

3rd(orange), 4th(magenta), and 5th(purple) order respectively. Interestingly we found that the expansion till the 2nd order, i.e. the series with $(\tilde{\mu}-\tilde{\mu_c})^2$ and $(\tilde{\mu}-\tilde{\mu_c})^4$ terms only, agrees remarkably well with the full result up to very large $\tilde{\mu}$, indicating some fine cancellations among all higher order terms.

The expansion for the density is given by:

$$\tilde{d} = \sum_n f_{2n-1}\left(\tilde{\mu}-\tilde{\mu_c}\right)^{2n-1} \tag{42}$$

$$f_1 = \frac{3}{\pi}\,,\ f_3 = \frac{36\,\Gamma\left(\frac{13}{6}\right)}{\pi^{\frac{7}{2}}\,\Gamma\left(\frac{11}{3}\right)}\,,\ f_5 = \frac{729}{8\pi^6}\left[\frac{2\,\Gamma\left(\frac{13}{6}\right)^2}{\Gamma\left(\frac{8}{3}\right)^2} - \frac{\sqrt{\pi}\,\Gamma\left(\frac{23}{6}\right)}{\Gamma\left(\frac{13}{3}\right)}\right]\,,\ \ldots$$

Again we skip to show the higher order coefficients and give an idea of the numbers: $f_1 = 0.95493$, $f_3 = 0.176709$, $f_5 = 0.00945598$, $f_7 = -0.00292787$, $f_9 = 0.000107106$. From the expansion it is clear that there is a jump in the slope of $\tilde{d}$ versus μ, i.e. 0 at $\tilde{\mu} \to \tilde{\mu_c}^-$ and $\frac{3}{\pi}$ at $\tilde{\mu} \to \tilde{\mu_c}^+$. We also note that these coefficients are related to those in the pressure expansion by $f_{2n-1} = (2n)\cdot c_{2n}$ order by order as required by $\tilde{d} = \partial_{\tilde{\mu}}\tilde{P}$. In Fig.2(right) we compare the full numerical result of the density (solid blue line) with its Taylor series results truncated at the 1st(red), 2nd(green), 3rd(orange), 4th(magenta), and

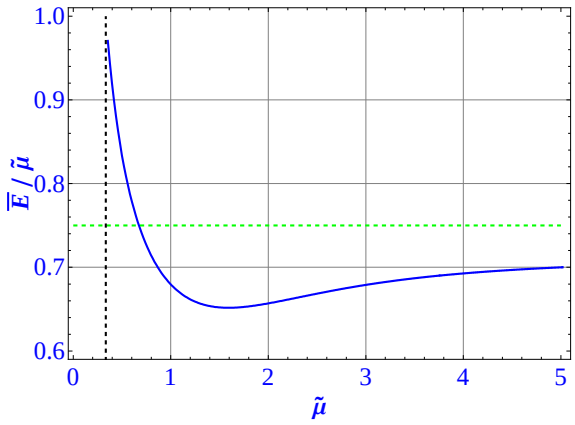

Figure 3: The energy per particle versus chemical potential. The horizontal dashed green line indicates the free value. The vertical dashed black line indicates the position of the phase transition.

5th(purple) order respectively. Not surprisingly we again found that the expansion till the 2nd order, i.e. the series with $(\tilde{\mu}-\tilde{\mu_c})$ and $(\tilde{\mu}-\tilde{\mu_c})^3$ terms only, agrees remarkably well with the full result up to very large $\tilde{\mu}$.

Finally we study another quantity of interest, i.e. the energy per particle $\bar{E}$ which at $T=0$ is given by $\bar{E}=(\tilde{\mu}\tilde{d}-\tilde{P})/\tilde{d}\equiv g(\tilde{\mu})\tilde{\mu}$. The function $g(\tilde{\mu})$ is plotted in Fig.3 as solid blue line. The dashed green line indicates the free case $g=3/4$. We see that close to the transition point the energy per particle deviates much from the free value and drops very sharply, while at much larger density it curves back and approaches the free value from below very slowly. We notice that the curve crosses the free line at about $\tilde{\mu}\approx 2\tilde{\mu_c}$: it may imply that below this density the system has repulsive interaction and above it the system has attractive interaction. In either regions, the deviation of $\bar{E}$ from free case is rather modest.

We also present the results with physical scales recovered as in Eq.(33)

$$\begin{aligned} P &= \frac{1}{2\cdot 3^8\cdot\pi^5}\times N_s\times N_f\times N_c\times(\lambda^3 M_{KK}^4)\times\sum_n\frac{c_{2n}}{3^{2n}}\left(\frac{\mu}{\mu_c}-1\right)^{2n} \\ &= N_s\times N_f\times N_c\times(\frac{\mu_c^4}{2\pi\lambda})\times\sum_n\frac{c_{2n}}{3^{2n-4}}\left(\frac{\mu}{\mu_c}-1\right)^{2n} \end{aligned} \tag{43}$$

and

$$D_{2n} \equiv \frac{\partial^{2n}(P/\mu_c^4)}{\partial(\mu/\mu_c)^{2n}}\Big|_{\mu=\mu_c} = N_s \times N_f \times N_c \times \frac{c_{2n}(2n)!}{3^{2n-4}(2\pi)} \times \frac{1}{\lambda} \tag{44}$$

where we have used $\mu_c = \frac{u_{KK}}{3} = \frac{\lambda M_{KK}}{27\pi}$.

6. Summary and Discussions

In summary, we have calculated the baryonic density and susceptibilities in a holographic model of QCD. The results both for the hot QGP phase in Eq.(34) and for the cold dense phase in Eq.(44) show interesting patterns due to strong coupling dynamics. In the following we discuss relevant lessons for QCD that can be learned from the results.

We first discuss the results for hot QGP phase close to T_c. To give an idea of the numbers, we re-write the results in Eq.(34) as:

$$\frac{d_2}{N_s N_f N_c} \approx 0.012 \cdot \lambda\tilde{T} \ , \quad \frac{d_4}{N_s N_f N_c} \approx \frac{0.37}{\lambda\tilde{T}} \ , \quad \frac{d_6}{N_s N_f N_c} \approx -\frac{26}{\lambda^3\tilde{T}^3} \tag{45}$$

We first note that a few qualitative features agree well with the lattice QCD data shown in Fig.1: the sign pattern of $d_{2,4,6}$ is the same, d_2 approximately exhibits linear growth with T close to T_c while $d_{4,6}$ shows quick decrease with T, and also d_6 vanishes much more abruptly than d_4. If one takes a $\lambda \sim 10 - 20$,[4] our d_2 values are very close to the lattice results, but the d_4 and d_6 values are too small. The comparison seems to indicate that dynamics from very strong coupling of *quarks only* tends to suppress higher order susceptibilities and may not be adequate to account for the $d_{4,6}$ close to T_c seen in lattice QCD: this is yet another indication that those higher order susceptibilities may be attributed to multi-quark correlations like baryons which manifest themselves more and more in higher order susceptibilities as we already pointed out in Section.II.

Another interesting observation is that for both phases we have noticed that in the dense regime the energy per particle $\bar{E}$ is very close to the Stefan-Boltzmann limit, i.e. $\frac{\bar{E}}{\bar{E}_{SB}}$ (the so-called Bertsch number) is close to 1 despite the strong coupling. We remind that the result of entropy in D3-D7 system (roughly involving adjoint gauge sector but without fundamental fermions)

[4] $\lambda \sim 17$ from [31].

deviates from the Stefan-Boltzmann limit by 25%. This comparison indicates that the strong coupling dynamics may somehow modify the thermodynamics of fundamental fermions much more mildly than of the gauge fields. Interestingly lattice QCD seems to show similar situation: while d_2 approaches the Stefan-Boltzmann limit already around $1.4T_c$, the pure gauge lattice results show no tendency toward the same limit even at $4T_c$.

Finally we point out that the cold dense phase of the Sakai-Sugimoto model studied above has its many features similar to the quarkyonic matter in large N_c QCD [23][24]. Both are in the confined regime but have their thermodynamics scaling as $N_c N_f$ like a quark system. The transition from the vacuum phase to the dense phase for both happens at about the baryon mass threshold as a second order one, after which the baryonic density starts growing. While calculation is hard for the quarkynoic matter in QCD, one may study its holographic dual quantitatively and obtain useful results as ours in Section.V. It will be very interesting to further investigate via the holographic method the many interesting features of the quarkyonic matter, e.g. the chiral symmetry and excitations near or deep into the Fermi surface, etc, which were previously qualitatively studied.

Acknowledgements: We thank Ismail Zahed, Sang-Jin Sin, Andrei Parnachev, and Matthew Lippert for discussions. JL is also grateful to Volker Koch and Larry McLerran for helpful discussions. JL is supported by the Director, Office of Energy Research, Office of High Energy and Nuclear Physics, Divisions of Nuclear Physics, of the U.S. Department of Energy under Contract No. DE-AC02-05CH11231. KK is supported in part by US-DOE grants DE-FG02-88ER40388 and DE-FG03-97ER4014.

A. The Background Metric Generated by D4 branes

In this appendix we summarize the metric generated by N_c D4 branes presented in [51].

At zero temperature, the metric generated by N_c D4-branes are given by

$$ds^2 = \left(\frac{U}{R}\right)^{3/2}\left(-(dX_0)^2 + (d\vec{X})^2 + f(U)(dX_4)^2\right) + \left(\frac{R}{U}\right)^{3/2}\left(\frac{dU^2}{f(U)} + U^2 d\Omega_4^2\right) \ ,$$

where

$$f(U) \equiv 1 - \frac{U_{\rm KK}^3}{U^3} \ . \tag{46}$$

$\vec{X} = X_{1,2,3}$, while $U(\geq U_{KK})$ and Ω_4 are the radial coordinate and four angle variables in the $X_{5,6,7,8,9}$ direction. R is given by

$$R^3 \equiv \pi g_s N_c l_s^3 \ , \tag{47}$$

where g_s and l_s are the string coupling and length respectively. Since X_4 is compacitified to a circle, to avoid a conical singularity at $U = U_{\rm KK}$, the period of δX_4 is set to

$$\delta X_4 = \frac{4\pi}{3} \frac{R^{3/2}}{U_{\rm KK}^{1/2}} \ . \tag{48}$$

The field theory is defined by Kaluza-Klein mass ($M_{\rm KK}$) and the four-dimensional coupling constant at the compactification scale, g_{YM},

$$M_{\rm KK} \equiv \frac{2\pi}{\delta X_4} = \frac{3}{2} \frac{U_{\rm KK}^{1/2}}{R^{3/2}} \ , \qquad g_{YM}^2 = \frac{g_5^2}{\delta X_4} = 2\pi M_{\rm KK} g_s l_s \ . \tag{49}$$

where $g_5 (= (2\pi)^2 g_s l_s)$ is the five dimensional coupling constant obtained from D4 brane DBI action. From (47) and (49) the parameters R, $U_{\rm KK}$, and g_s may be expressed in terms of $M_{\rm KK}$, $l (= g_{YM}^2 N_c)$, and l_s as

$$R^3 = \frac{l l_s^2}{2 M_{\rm KK}} \ , \quad U_{\rm KK} = \frac{2}{9} l M_{\rm KK} l_s^2 \ , \quad g_s = \frac{l}{2\pi M_{\rm KK} N_c l_s} \ . \tag{50}$$

At finite temperature, there are two possibilities [52]. One is to follow the standard prescription of the finite temperature field theory. The geometry is the same as the zero temperature apart from the fact that the time direction is Euclidean ($X_0 \to X_0^E = i X_0$) and compactified with a circumference $\beta = 1/T$:

$$\begin{aligned} ds^2 = & \left(\frac{U}{R}\right)^{3/2} \left((dX_0^E)^2 + (d\vec{X})^2 + f(U)(dX_4)^2 \right) \\ & + \left(\frac{R}{U}\right)^{3/2} \left(\frac{dU^2}{f(U)} + U^2 d\Omega_4^2 \right) \ , \end{aligned}$$

This corresponds to the confined phase which is thermodynamically preferred (i.e. with the smallest action) in the low temperature regime. The other possible geometry contains the black hole, which is another saddle point of the Euclidean path integral over supergravity configuration. The pertinent background is

$$ds^2 = \left(\frac{U}{R}\right)^{3/2}\left(f(U)(dX_0^E)^2 + (d\vec{X})^2 + (dX_4)^2\right) + \left(\frac{R}{U}\right)^{3/2}\left(\frac{dU^2}{f(U)} + U^2 d\Omega_4^2\right) \ ,$$

where[5]

$$f(U) \equiv 1 - \frac{U_T^3}{U^3} \ . \tag{51}$$

This corresponds to deconfined phase which is thermodynamically preferred (i.e. with the smallest action) at high temperature. To avoid a conical singularity at $U = U_T$ the period of δX_0^E of the compactified t_E direction is set to

$$\delta X_0^E = \frac{4\pi}{3}\left(\frac{R^3}{U_T}\right)^{1/2} \equiv \frac{1}{T} \equiv \beta \ , \tag{52}$$

which is identified with the inverse temperature. The confinement/deconfinement phase transition, i.e. the switching from one background geometry to the other, occurs when $\delta X_4 = \delta X_0^E$ *i.e.* at the critical temperature T_c,

$$T_c = \frac{M_{\rm KK}}{2\pi} \ . \tag{53}$$

References

[1] See e.g.: J. H. Schwarz, arXiv:0708.1917 [hep-th].

[2] J. M. Maldacena, Adv. Theor. Math. Phys. **2**, 231 (1998) [Int. J. Theor. Phys. **38**, 1113 (1999)] [arXiv:hep-th/9711200].

[5]Strictly speaking we need to use the different notation to distinguish (51) from (46). However for notational convenience we will use the same notation. It will not make any confusion since the meaning will be clear from the context.

[3] S. S. Gubser, I. R. Klebanov and A. M. Polyakov, Phys. Lett. B **428**, 105 (1998) [arXiv:hep-th/9802109].

[4] E. Witten, Adv. Theor. Math. Phys. **2**, 253 (1998) [arXiv:hep-th/9802150].

[5] O. Aharony, S. S. Gubser, J. M. Maldacena, H. Ooguri and Y. Oz, Phys. Rept. **323**, 183 (2000) [arXiv:hep-th/9905111].

[6] K. Peeters and M. Zamaklar, Eur. Phys. J. ST **152**, 113 (2007) [arXiv:0708.1502 [hep-ph]].

[7] D. Mateos, Class. Quant. Grav. **24**, S713 (2007) [arXiv:0709.1523 [hep-th]].

[8] J. Erdmenger, N. Evans, I. Kirsch and E. Threlfall, Eur. Phys. J. A **35**, 81 (2008) [arXiv:0711.4467 [hep-th]].

[9] L. F. Alday and R. Roiban, Phys. Rept. **468**, 153 (2008) [arXiv:0807.1889 [hep-th]].

[10] S. S. Gubser and A. Karch, arXiv:0901.0935 [hep-th].

[11] S. S. Gubser, S. S. Pufu, F. D. Rocha and A. Yarom, arXiv:0902.4041 [hep-th].

[12] M. Rangamani, arXiv:0905.4352 [hep-th].

[13] F. Karsch, Lect. Notes Phys. **583**, 209 (2002) [arXiv:hep-lat/0106019].

[14] E. V. Shuryak, Prog. Part. Nucl. Phys.53:273-303,2004; Nucl. Phys. A **750**, 64 (2005). M. Gyulassy and L. McLerran, Nucl. Phys. A **750**, 30 (2005) [arXiv:nucl-th/0405013].

[15] E. V. Shuryak, Prog. Part. Nucl. Phys. **62**, 48 (2009).

[16] D. E. Kharzeev, arXiv:0902.2749 [hep-ph].

[17] S. S. Gubser, I. R. Klebanov and A. W. Peet, Phys. Rev. D **54**, 3915 (1996) [arXiv:hep-th/9602135].

[18] G. Policastro, D. T. Son and A. O. Starinets, Phys. Rev. Lett. **87**, 081601 (2001); P. Kovtun, D. T. Son and A. O. Starinets, Phys. Rev. Lett. **94**, 111601 (2005).

[19] R. Rapp, T. Schafer, E. V. Shuryak and M. Velkovsky, Phys. Rev. Lett. **81**, 53 (1998) [arXiv:hep-ph/9711396]. M. G. Alford, K. Rajagopal and F. Wilczek, Phys. Lett. B **422**, 247 (1998) [arXiv:hep-ph/9711395].

[20] M. G. Alford, K. Rajagopal and F. Wilczek, Nucl. Phys. B **537**, 443 (1999) [arXiv:hep-ph/9804403].

[21] J. Berges and K. Rajagopal, Nucl. Phys. B **538**, 215 (1999) [arXiv:hep-ph/9804233].

[22] J. Liao and P. Zhuang, Phys. Rev. D **68**, 114016 (2003) [arXiv:cond-mat/0307516]; Chin. Phys. Lett. **19**, 177 (2002).

[23] L. McLerran and R. D. Pisarski, Nucl. Phys. A **796**, 83 (2007) [arXiv:0706.2191 [hep-ph]].

[24] L. McLerran, K. Redlich and C. Sasaki, Nucl. Phys. A **824**, 86 (2009) [arXiv:0812.3585 [hep-ph]].

[25] V. Koch, arXiv:0810.2520 [nucl-th]. V. Koch, A. Majumder and J. Randrup, Phys. Rev. Lett. **95**, 182301 (2005) [arXiv:nucl-th/0505052].

[26] C. R. Allton *et al.*, Phys. Rev. D **71**, 054508 (2005) [arXiv:hep-lat/0501030].

[27] M. Cheng *et al.*, Phys. Rev. D **79**, 074505 (2009) [arXiv:0811.1006 [hep-lat]].

[28] R. V. Gavai and S. Gupta, Phys. Rev. D **71**, 114014 (2005) [arXiv:hep-lat/0412035]; R. V. Gavai and S. Gupta, Phys. Rev. D **72**, 054006 (2005) [arXiv:hep-lat/0507023]; Phys. Rev. D **78**, 114503 (2008) [arXiv:0806.2233 [hep-lat]].

[29] C. Bernard *et al.*, Phys. Rev. D **77**, 014503 (2008) [arXiv:0710.1330 [hep-lat]].

[30] A. Hietanen and K. Rummukainen, JHEP **0804**, 078 (2008) [arXiv:0802.3979 [hep-lat]].

[31] T. Sakai and S. Sugimoto, Prog. Theor. Phys. **113**, 843 (2005) [arXiv:hep-th/0412141]; T. Sakai and S. Sugimoto, Prog. Theor. Phys. **114**, 1083 (2005) [arXiv:hep-th/0507073].

[32] H. Hata, T. Sakai, S. Sugimoto and S. Yamato, arXiv:hep-th/0701280; H. Hata, M. Murata and S. Yamato, Phys. Rev. D **78**, 086006 (2008) [arXiv:0803.0180 [hep-th]]; K. Hashimoto, T. Sakai and S. Sugimoto, Prog. Theor. Phys. **120**, 1093 (2008) [arXiv:0806.3122 [hep-th]]; D. K. Hong, M. Rho, H. U. Yee and P. Yi, JHEP **0709**, 063 (2007) [arXiv:0705.2632 [hep-th]]; K. Y. Kim and I. Zahed, JHEP **0809**, 007 (2008) [arXiv:0807.0033 [hep-th]]; K. Nawa, H. Suganuma and T. Kojo, Phys. Rev. D **75**, 086003 (2007) [arXiv:hep-th/0612187].

[33] K. Y. Kim and I. Zahed, JHEP **0903**, 131 (2009) [arXiv:0901.0012 [hep-th]]. K. Hashimoto, T. Sakai and S. Sugimoto, arXiv:0901.4449 [hep-th]; Y. Kim, S. Lee and P. Yi, arXiv:0902.4048 [hep-th]; P. Yi, arXiv:0902.4515 [hep-th].

[34] O. Aharony, J. Sonnenschein and S. Yankielowicz, Annals Phys. **322**, 1420 (2007) [arXiv:hep-th/0604161]; A. Parnachev and D. A. Sahakyan, Phys. Rev. Lett. **97**, 111601 (2006) [arXiv:hep-th/0604173]; K. Peeters, J. Sonnenschein and M. Zamaklar, Phys. Rev. D **74**, 106008 (2006) [arXiv:hep-th/0606195].

[35] K. Y. Kim, S. J. Sin and I. Zahed, arXiv:hep-th/0608046; N. Horigome and Y. Tanii, JHEP **0701**, 072 (2007) [arXiv:hep-th/0608198]; A. Parnachev and D. A. Sahakyan, Nucl. Phys. B **768**, 177 (2007) [arXiv:hep-th/0610247]; M. Rozali, H. H. Shieh, M. Van Raamsdonk and J. Wu, JHEP **0801**, 053 (2008) [arXiv:0708.1322 [hep-th]]; J. L. Davis, M. Gutperle, P. Kraus and I. Sachs, JHEP **0710**, 049 (2007) [arXiv:0708.0589 [hep-th]]; K. Y. Kim, S. J. Sin and I. Zahed, JHEP **0809**, 001 (2008) [arXiv:0712.1582 [hep-th]]; K. Y. Kim, S. J. Sin and I. Zahed, JHEP **0807** (2008) 096 [arXiv:0803.0318 [hep-th]]; K. Y. Kim and I. Zahed, JHEP **0812** (2008) 075 [arXiv:0811.0184 [hep-th]]; K. Nawa, H. Suganuma and T. Kojo, Phys. Rev. D **79**, 026005 (2009) [arXiv:0810.1005 [hep-th]].

[36] O. Bergman, G. Lifschytz and M. Lippert, JHEP **0711**, 056 (2007) [arXiv:0708.0326 [hep-th]].

[37] K. Y. Kim, S. J. Sin and I. Zahed, JHEP **0801**, 002 (2008) [arXiv:0708.1469 [hep-th]].

[38] J. Liao and E. V. Shuryak, Phys. Rev. D **73**, 014509 (2006) [arXiv:hep-ph/0510110].

[39] M. Cheng *et al.*, Phys. Rev. D **77**, 014511 (2008) [arXiv:0710.0354 [hep-lat]].

[40] H. B. Meyer, Phys. Rev. D **76**, 101701 (2007).

[41] O. Kaczmarek and F. Zantow, Phys. Rev. D **71**, 114510 (2005) [arXiv:hep-lat/0503017]; arXiv:hep-lat/0506019.

[42] S. Datta, F. Karsch, P. Petreczky and I. Wetzorke, `hep-lat/0403017`; M. Asakawa and T. Hatsuda, `hep-lat/0308034`.

[43] J. Liao and E. Shuryak, Phys. Rev. C **75**, 054907 (2007); Phys. Rev. Lett. **101**, 162302 (2008); Phys. Rev. C **77**, 064905 (2008); arXiv:0804.4890 [hep-ph]; Phys. Rev. Lett. **102**, 202302 (2009) [arXiv:0810.4116 [nucl-th]].

[44] M. N. Chernodub and V. I. Zakharov, Phys. Rev. Lett. **98**, 082002 (2007) [arXiv:hep-ph/0611228].

[45] A. D'Alessandro and M. D'Elia, Nucl. Phys. B **799**, 241 (2008).

[46] C. Ratti and E. Shuryak, arXiv:0811.4174 [hep-ph].

[47] E.V. Shuryak and I. Zahed, Phys. Rev. C **70**, 021901 (2004).

[48] E. V. Shuryak and I. Zahed, Phys. Rev. D **70**, 054507 (2004).

[49] J. Liao and E. V. Shuryak, Nucl. Phys. A **775**, 224 (2006) [arXiv:hep-ph/0508035].

[50] C. Ratti, M. A. Thaler and W. Weise, Phys. Rev. D **73**, 014019 (2006) [arXiv:hep-ph/0506234].

[51] M. Kruczenski, D. Mateos, R. C. Myers and D. J. Winters, JHEP **0405**, 041 (2004) [arXiv:hep-th/0311270].

[52] E. Witten, Adv. Theor. Math. Phys. **2**, 505 (1998) [arXiv:hep-th/9803131].